

R3 STORE



CCLRC Library & Info Services



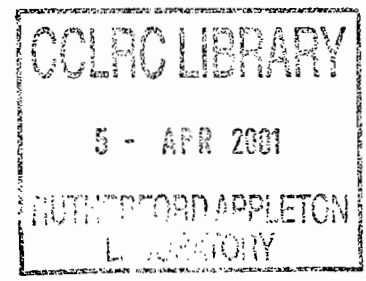
C4051485

**Technical Report**  
RAL-TR-2001-021

# Scattering by Entangled Spatial and Spin Degrees of Freedom

E B Karlsson and S W Lovesey

3<sup>rd</sup> April 2001



© Council for the Central Laboratory of the Research Councils 2001

Enquiries about copyright, reproduction and requests for additional copies of this report should be addressed to:

The Central Laboratory of the Research Councils  
Library and Information Services  
Rutherford Appleton Laboratory  
Chilton  
Didcot  
Oxfordshire  
OX11 0QX  
Tel: 01235 445384 Fax: 01235 446403  
E-mail [library@rl.ac.uk](mailto:library@rl.ac.uk)

**ISSN 1358-6254**

Neither the Council nor the Laboratory accept any responsibility for loss or damage arising from the use of information contained in any of their reports or in any communication about their tests or investigations.

# Scattering by entangled spatial and spin degrees of freedom

E. B. Karlsson<sup>1</sup> and S. W. Lovesey<sup>2</sup>

<sup>1</sup>Department of Physics, Uppsala University, P. O. Box 530, SE-75121 Uppsala, Sweden

<sup>2</sup>Rutherford-Appleton Laboratory, Oxfordshire, OX11 0QX, UK

PACs: 61.12 Bt, Theories of diffraction and scattering  
03.65 Bz, Foundations, theory of measurements

email:

E. B. Karlsson: [erk@fysik.uu.se](mailto:erk@fysik.uu.se)

S.W.Lovesey: [S.W.Lovesey@rl.ac.uk](mailto:S.W.Lovesey@rl.ac.uk)

## Scattering by entangled spatial and spin degrees of freedom

E. B. Karlsson, Department of Physics, Uppsala University,  
P.O. Box 530, S-75121 Uppsala, Sweden.

S. W. Lovesey, Rutherford Appleton Laboratory,  
Oxfordshire, OX11 0QX, UK.

### Abstract

Several recent experiments on liquid and solid samples containing protons or deuterons show an interesting anomaly, which is a shortfall in the intensity of energetic neutrons scattered by the samples. Previously we demonstrated that quantum correlations in the spatial and spin degrees of freedom of the hydrogen isotopes lead to entanglement in scattering and a reduction in the scattered intensity. The viability of short-lived quantum correlations as the cause of the observed anomalies is further explored and found to be entirely feasible. General features of the basic premiss, that quantum entanglement reduces the scattered signal, are discussed and the interpretation of the neutron scattering experiments is set in context to related work on other systems. For the experiments in question, the duration of a scattering event,  $\tau_s$ , is a fraction of a femtosecond which is extremely short compared to solid-state relaxation times. Increasing  $\tau_s$ , by suitably changing experimental conditions, restores the intensity to the standard value calculated from the single atom cross-section and concentration of particles. Our physical picture of the restoration is evolution with increasing  $\tau_s$  from a pure state of the particles (described by a wavefunction) to a mixed state (described by a density matrix) that is created, through decoherence, by steadily engaging the solid-state environment of the particles.

## 1. Introduction

The intensity of energetic neutrons inelastically scattered by samples loaded with one of the isotopes of hydrogen is found to be smaller than expected from an application of the standard approach to the theory of scattering. For protons the shortfall in intensity can be as much as 40%, and for deuterons the shortfall is about 10% [1, 2]. The search for an explanation of the observed shortfall in intensity has led to a consideration of the influence on the intensity of quantum correlations between particles in a sample, and the entanglement of degrees of freedom that appear in the scattering of radiation.

We refer to the purely quantum mechanical correlations between identical particles, which is an effect created by the behaviour of the wavefunction with respect to exchange of pairs of particles. (Exchange of a pair of bosons (particles with integer spin) leaves their wavefunction unchanged, while exchange of a pair of fermions (particles with half-integer spin) changes the sign of their wavefunction.) One well-established example of the influence of the quantum correlations, which is also called an exchange effect, is seen in scattering of identical particles, e.g. in collisions of inert gas atoms (spin-zero particles) or electrons (spin- $\frac{1}{2}$  particles). In this instance, the exchange effect appears as an interference between the two channels of scattering in which a particle is deflected through angles  $\theta$  and  $\pi - \theta$ . If the behaviour of the wavefunction with respect to exchange of particles is neglected the calculated collision cross-section is just an incoherent sum of the cross-sections for deflection through  $\theta$  and  $\pi - \theta$ . A second example is found in the formation of ortho and para-states of the hydrogen molecule. Not surprisingly, perhaps, the two states are distinguished in neutron scattering by offering quite different cross-sections.

Several aspects of the neutron-scattering experiments on samples loaded with protons or deuterons indicate that a quantum effect is the likely cause of the shortfall in intensity. For one thing, the size of the shortfall decreases with increasing mass of the target particles. We have given figures for protons and deuterons, and no shortfall in intensity has been reported for particles heavier than a deuteron. A second notable aspect of the experiments is the extremely short duration of the collision between an

The present paper contains four main sections. In section 2 we briefly review the neutron Compton scattering experiments that are at the heart of our work. Sections 3 and 4 are given over to discussions of quantum entanglement in condensed matter and its influence on the intensity of neutron Compton scattering. The last main section contains work aimed at interpreting the influence of entanglement in scattering events, and estimates of the size of the shortfall in scattering that can be realized with samples loaded with protons and deuterons.

## 2. Scattering by condensed matter; experimental details

Anomalies in neutron Compton scattering by hydrogen in condensed matter have been observed in condensed matter systems of a quite different nature; namely, water [6], metal hydrides [1, 2] and polymers [5].

The anomalies are seen as reductions in the cross-section of protons of between 10 and 30 percent (and smaller anomalies for deuterons) relative to the expected, tabulated values for isolated protons. The cross-sections have been obtained by comparing intensities for proton (H), or deuteron (D), peaks with those of heavier elements (X) in compounds with well-known stoichiometric ratios  $XH_x$ , etc.

All the above mentioned experiments have been performed in the same experimental setup, the eVS-spectrometer at the ISIS Facility, Rutherford Appleton Laboratory, UK. This spectrometer distinguishes scattering from H, D, etc. as separated peaks in the time-of-flight spectrum of the neutrons. Some of these anomalies, those observed in  $NbH_x$  and  $PdH_x$ , show up only at momentum transfers  $k$  that are very large while anomalies for water and the solid polystyrene are almost independent of  $k$ . As was shown in ref. [1], there is a one-to-one correspondence between the angle  $\theta$  through which the neutron beam is deflected and the duration of the scattering event  $\tau_s$ . Times  $\tau_s$  fall in the range  $10^{-16} - 10^{-15}$ s and the  $\theta$  –dependence of the intensities for H in  $NbH_x$  and  $PdH_x$  shows that shortfalls in the cross-section exist only for durations shorter than  $\sim 5 \times 10^{-15}$ s. The dependence of the cross-section ratio  $\sigma_H/\sigma_{Nb}$  for  $NbH_{0.8}$  as a function of  $\tau_s$  is shown in Fig. 1.

Observed structures in the scattered neutron intensity, which might be of the same origin as the anomalous cross-sections mentioned above, have also been reported using neutrons of intermediate energy  $\approx 0.5$  eV in the MARI spectrometer at the ISIS Facility [7]. The intensity from the compound  $\text{KHCO}_3$  exhibits a structure with extra components which indicate a (quantum mechanical) coupling between the two closely spaced protons in this compound. In an accompanying theoretical paper [8], Fillaux has discussed observed features in terms of correlated proton states. Two-body entanglement of fermionic and bosonic modes was also considered earlier for explaining Raman scattering on water [9].

In the eVS spectrometer, used for neutron Compton scattering, energy selection is made on the outgoing scattered neutrons, using resonance absorption in a metallic foil [10]. An important parameter for the interpretation of experiments using this inverse geometry type of spectrometer is the coherence length  $l_{\text{coh}} = \lambda^2/2\Delta\lambda$  of the neutron waves. The energy of the outgoing neutrons, selected by a 197–Au foil, is 4.91 eV which corresponds to a deBroglie-wavelength of  $\lambda = 9.04 \text{ E}^{-1/2} = 0.13\text{\AA}$ . The width of the resonance  $\Delta E = 0.26$  eV, which relates to a wavelength spread of  $\Delta\lambda = (1/2)9.04 \text{ E}^{-3/2}|\Delta E| = 0.0034\text{\AA}$ . The coherence length of the outgoing neutrons is therefore of the order of  $l_{\text{coh}} = 2.5 \text{ \AA}$ . Thus, although the wavelength of the neutrons is smaller than typical distances between two neighbouring hydrogen ions in the metal lattices ( $d \approx 2\text{\AA}$ ) there is still longitudinal coherence such that more than one scattering center can contribute to neutron scattering.

Interference in neutron Compton scattering is also taken into account in the work of Andreani et al. [11] on the  $\text{H}_2$  and  $\text{D}_2$  molecules. The authors analyse measurements, using the same Au–197 resonance for selecting the energy of neutrons in the eVS-spectrometer, with momentum transfers in the range  $30 - 60 \text{ \AA}^{-1}$ . Interference is considered for scattering from protons (or deuterons) within the same molecule, but not for particles belonging to different molecules. Their scattering situation is not the same as the one presently considered since the kinematics is different, with the whole molecule recoiling and with no dissociation possible within the momentum transfer range considered. In the model we discuss, the scattering particles are bound in a lattice and although both can contribute to the scattering amplitude, only one particle recoils.

### 3. Local entanglement in condensed matter

It is well known that in order to explain the thermal neutron scattering for molecular hydrogen it is necessary to take into account the symmetry of the two-proton wavefunction, which for these indistinguishable particles is determined by their fermionic character. This leads to completely different cross-sections for parahydrogen (with  $J = 0$  and the spatial part of the wavefunction symmetric under exchange of the particles) and orthohydrogen (with  $J = 1$  and spatial part antisymmetric).

In light molecules containing hydrogen, like compounds of the type  $XH_4$ , the fermionic character of wavefunctions also leads to a modification of the proton cross-section in thermal neutron scattering, but only of the order of a few percent as compared to independent proton values [12]. In these molecules, as well as in  $H_2$  and  $D_2$ , such exchange effects are reduced with increasing temperatures when molecules are excited to different configurations [13, 14].

On the other hand, in condensed systems (with the exception of superfluids), the spins of constituent nuclei are usually treated as randomly orientated and uncorrelated. This is considered to be valid even for identical nuclei, such as protons in metal hydrides or in hydrocarbon compounds. In theoretical predictions of scattering cross-sections they are therefore considered as individual scattering objects and the total cross-sections are calculated starting from a (coherent or incoherent, depending on the experimental situation) summation of scattering amplitudes from particles localized at definite sites.

It seems that it is this tacit assumption about the absence of nuclear correlations in condensed systems that should be abandoned in order to explain the measured cross-sections for neutron Compton scattering (NCS) in the metallic hydrides. As already mentioned, this type of scattering differs from thermal neutron scattering in the important aspect that the duration  $\tau_s$  of the scattering event in NCS is much shorter than



that occurring with thermal neutrons and typically  $\tau_s < 10^{-15}$ s. Entanglement between distant particles, which is expected to be extremely short-lived because of the high probability of decoherence created by the solid-state environment, may therefore be observed in NCS, although it has a negligible effect in thermal neutron scattering.

There exist estimates in the literature [15] of the decoherence time for quantum entangled macroscopic objects, exposed to collisions by particles or excitations. If these relations permit an extrapolation down to linear extensions of the order of a few Å and to the limit of single collisions (by phonons), the results for the decoherence time will fall in the range of  $10^{-16}$ s [1], which is of the same order of magnitude as  $\tau_s$  in NCS. These considerations have encouraged us to build a simple model for neutron Compton scattering which is based on systems of quantum-entangled particles in solid materials (for particles heavier than protons or deuterons effects of local entanglement will be much less pronounced in the time window currently accessible for measurements).

#### 4. A soluble model of scattering by identical particles

By restricting our attention to two particles in the sample we have a model of scattering which can be solved without approximation. As we mentioned in the introduction, overlap and direct interactions between the two particles are excluded, so correlations in the model are exclusively due to the purely quantum mechanical entanglements of spatial and spin degrees of freedom.

The particles are identical and we label them by  $\alpha$  and  $\beta$ . Their spins are denoted by  $I_\alpha$  and  $I_\beta$  and they are of magnitude  $I$ . The spin states are coupled, by a Clebsch-Gordan coefficient, to form a state with total angular momentum  $J$  and projection  $M$ . Such a state is represented by the spinor,

$$\chi_M^J(\alpha, \beta) = \sum_{mn} (I_\alpha m I_\beta n | JM) \left| I_\alpha m \right\rangle \left| I_\beta n \right\rangle. \quad (4.1)$$

One finds  $\chi_M^J(\beta, \alpha) = (-1)^{2I+J} \chi_M^J(\alpha, \beta)$ .

The total wavefunction is the product of  $\chi_M^J(\alpha, \beta)$  and a spatial wavefunction, in keeping with the nonrelativistic limit of quantum mechanics. Under exchange of the two particles, the total wavefunction is required to be symmetric for bosons and antisymmetric for fermions, i.e. exchanging the particles introduces in the total wavefunction a phase factor  $(-1)^{2I}$ . From our knowledge of the behaviour with respect to exchange of the spinor we find that, with respect to exchange of the two particles the spatial wavefunction acquires a phase  $(-1)^J$ .

In our model, there are two spatial centres, labelled 1 and 2. The one-particle spatial orbitals,  $\varphi_1(\mathbf{R})$  and  $\varphi_2(\mathbf{R})$ , are taken to be purely real (and thus non-degenerate) and to satisfy,

$$\int d\mathbf{R} \varphi_1^2(\mathbf{R}) = \int d\mathbf{R} \varphi_2^2(\mathbf{R}) = 1, \quad \text{with,} \quad \int d\mathbf{R} \varphi_1(\mathbf{R})\varphi_2(\mathbf{R}) = 0. \quad (4.2)$$

If the two centres are connected by the vector  $\mathbf{d}$ , one can use the representations  $\varphi_1(\mathbf{R}) = \varphi(\mathbf{R})$  and  $\varphi_2(\mathbf{R}) = \varphi(\mathbf{R} - \mathbf{d})$  and sensibly describe 1 (2) as the left (right) centre in the model. Suitably normalized, the spatial wavefunction of the initial state of the two particles is,

$$\frac{1}{\sqrt{2}} \left\{ \varphi_1(\mathbf{R}_\alpha)\varphi_2(\mathbf{R}_\beta) + \zeta \varphi_1(\mathbf{R}_\beta)\varphi_2(\mathbf{R}_\alpha) \right\}. \quad (4.3)$$

Here,  $\zeta = (-1)^J$ . By using  $\zeta^2 = 1$  and the fact that a wavefunction is arbitrary to within a phase factor it is evident that, in (4.3) the phase factor  $\zeta$  can equally well appear in the first product of wavefunctions; with regard to the physics which (4.3) describes, the phase factor  $\zeta$  is not specifically attached to the first or second of the two product states.

The total wavefunction for the initial state of the two particles is the product of  $\chi_M^J(\alpha, \beta)$ , which is defined by (4.1), and the spatial wavefunction given in (4.3). On exchanging the two particles ( $\alpha \leftrightarrow \beta$ ) the total function acquires a factor  $(-1)^{2I}$  as

required in quantum mechanics applied to identical particles. Evidently, in this type of wavefunction, the spatial and spin degrees of freedom are not separable.

The total wavefunction for the final state of the two particles, after they have acquired energy and momentum from impinging neutrons, has the same structure as the initial total wavefunction. The spin state is represented by  $\chi_{M'}^{J'}(\alpha, \beta)$ . The associated spatial wavefunction is cognizant of the kinematics in Compton scattering. For the intensity as a function of energy to accumulate at the recoil energy of one particle it must contain a state which is a plane-wave, to a good approximation. Let the plane-wave be proportional to  $\exp(i\mathbf{p}' \cdot \mathbf{R})$  and denote the second one-particle orbital by  $\psi(\mathbf{R})$ . The plane-wave is normalized in a box, and  $\psi(\mathbf{R})$  is normalized to unity like  $\phi_1(\mathbf{R})$  and  $\phi_2(\mathbf{R})$ . The normalization box has a volume  $\Omega$  and the normalization factor with the plane-wave is eventually absorbed in a momentum wavefunction. The total final-state wavefunction is,

$$\frac{1}{\sqrt{2\Omega}} \left\{ \exp(i\mathbf{p}' \cdot \mathbf{R}_\alpha) \psi(\mathbf{R}_\beta) + \zeta' \exp(i\mathbf{p}' \cdot \mathbf{R}_\beta) \psi(\mathbf{R}_\alpha) \right\} \chi_{M'}^{J'}(\alpha, \beta), \quad (4.4)$$

where the phase factor  $\zeta' = (-1)^{J'}$ .

The spatial part of (4.4) is particular to the Compton limit of scattering. As we will shortly see, the plane-wave it contains strongly influences the calculated cross-section. Perhaps the best way of appreciating the influence of the plane-wave in the final state is to compare subsequent working, made for the extreme Compton limit expressed by (4.4), with results gathered in an appendix that are appropriate before reaching the Compton limit of scattering.

The cross-section for scattering is calculated using Fermi's prescription for a neutron-nuclear collision, namely, the Golden-Rule for transition rates and his pseudo-potential for the interaction operator. For two particles the neutron-nuclear potential is,

$$V = b_\alpha \exp(i\mathbf{k} \cdot \mathbf{R}_\alpha) + b_\beta \exp(i\mathbf{k} \cdot \mathbf{R}_\beta), \quad (4.5)$$

and the cross-section is proportional to  $|\langle \text{final} | V | \text{initial} \rangle|^2$ . The scattering-length operator,

$$b = A + B\mathbf{s} \cdot \mathbf{I}, \quad (4.6)$$

is independent of the position variable, and  $\mathbf{s}$  is the operator for the spin of the neutron ( $A$  and  $B$  are obtained from independent measurements). The spatial factors in  $V$  are functions of the wavevector transfer,  $\mathbf{k}$ , which is varied in the experiment. In the matrix element  $\langle \text{final} | V | \text{initial} \rangle$ , to be used in the Golden-Rule,  $b_\alpha$  and  $b_\beta$  act on spinors, and  $\exp(i\mathbf{k} \cdot \mathbf{R}_\alpha)$  and  $\exp(i\mathbf{k} \cdot \mathbf{R}_\beta)$  act on spatial wavefunctions.

Looking at the initial and final total wavefunctions and  $V$  we see that,  $\langle \text{final} | V | \text{initial} \rangle$  contains eight spatial matrix elements, four of the form,

$$\int d\mathbf{R}_\alpha \exp(i\mathbf{R}_\alpha \cdot \mathbf{k}) \psi^*(\mathbf{R}_\alpha) \varphi_1(\mathbf{R}_\alpha) \int d\mathbf{R}_\beta \exp(-i\mathbf{p}' \cdot \mathbf{R}_\beta) \varphi_2(\mathbf{R}_\beta). \quad (4.7)$$

and four of the form,

$$\int d\mathbf{R}_\alpha \exp\{i\mathbf{R}_\alpha \cdot (\mathbf{k} - \mathbf{p}')\} \varphi_1(\mathbf{R}_\alpha) T_2, \quad (4.8)$$

where,

$$T_2 = \int d\mathbf{R} \psi^*(\mathbf{R}) \varphi_2(\mathbf{R}). \quad (4.9)$$

Consider the first integral in (4.7). Because the magnitude of  $\mathbf{k}$  is very large the phase factor  $\exp(i\mathbf{R}_\alpha \cdot \mathbf{k})$  contains very many oscillations, between +1 and -1, as  $\mathbf{R}_\alpha$  varies in the volume of space in which  $\varphi_1(\mathbf{R}_\alpha)$  is appreciably different from zero; a volume which is the order of a unit cell in the crystal. In consequence, the integral in question is close to zero. The corresponding integral in (4.8) can be significantly different from zero when  $\mathbf{p}'$  is chosen close to  $\mathbf{k}$ , so  $\exp\{i\mathbf{R}_\alpha \cdot (\mathbf{k} - \mathbf{p}')\}$  has relatively few oscillations in a

unit cell. From the conservation of momentum it follows that  $\mathbf{p}' - \mathbf{k} = \mathbf{p}$  is the initial wavevector of the struck particle. With  $\mathbf{p}' \simeq \mathbf{k}$  the second integral in (4.7) is close to zero and the product of integrals in the expression can be safely neglected in comparison to (4.8). For the latter we write,  $K(\mathbf{p})T_2$ . Here, the momentum wavefunction,

$$K(\mathbf{p}) = \Omega^{-1/2} \int d\mathbf{R} \exp(-i\mathbf{R} \cdot \mathbf{p}) \varphi_1(\mathbf{R}) = \Omega^{-1/2} \int d\mathbf{R} \exp(-i\mathbf{R} \cdot \mathbf{p}) \varphi(\mathbf{R}),$$

satisfies,

$$\sum_{\mathbf{p}} |K(\mathbf{p})|^2 = \frac{\Omega}{(2\pi)^3} \int d\mathbf{p} |K(\mathbf{p})|^2 = 1.$$

The four terms in the matrix element of  $V$  that survive the Compton limit are,

$$\langle \text{final} | V | \text{initial} \rangle = \frac{1}{2} \chi_{M'}^J(\alpha, \beta) \{b_\alpha + \zeta \zeta' b_\beta\} \chi_M^J(\alpha, \beta) K(\mathbf{p}) \{T_2 + \zeta \exp(-i\mathbf{p} \cdot \mathbf{d}) T_1\} = K(\mathbf{p}) F(J' M', J M), \quad (4.10)$$

where  $T_1$  is defined in accord with (4.9) and the last equality defines  $F(J' M', J M)$ . The spatial phase-factor  $\exp(-i\mathbf{p} \cdot \mathbf{d})$  in (4.10) arises in the momentum wavefunction created from  $\varphi_2(\mathbf{R}) = \varphi(\mathbf{R} - \mathbf{d})$ .

Let us pause here and compare (4.10) with the corresponding expression in the calculation by Pitaevskii and Stringari [4] of Compton scattering by two identical Bose-Einstein condensates. Spin variables in this case play no part and only the spatial part of (4.10) is significant in the comparison. It reveals that the two model systems contain exactly the same spatial coherence, embodied here in  $\exp(-i\mathbf{p} \cdot \mathbf{d})$ , and  $\zeta$  in (4.10) appears in place of the unknown phase factor introduced on bringing together two condensates. The modulation with respect to  $\mathbf{p}$  of the Compton cross-section for two condensates, caused by the phase factor  $\exp(-i\mathbf{p} \cdot \mathbf{d})$ , is not observed in the neutron Compton scattering experiments [1, 2] and our expression for the total cross-section, to be derived from (4.10), is consistent with this observation.

In ref. [3], the final state was chosen to be orthogonal to the initial state. This was in order to show that even when the initial and final states of the particles are uncorrelated, cancellations still appear in the amplitudes that result from scattering on the two particles in the pair. Here, the calculation is first presented as in ref. [3]. Later, it is shown that inclusion of  $J'=J$ , terms that are excluded as in ref. [3], will lead to only a small correction for the proton pairs. For deuteron pairs, on the other hand, the  $J'=J$  terms could play a larger rôle.

The overlap of the initial and final states is obtained by following the steps that lead to (4.10) and, in fact, the result can simply be written down by inspection of (4.10). We find, following ref. [3],

$$\langle \text{final} | \text{initial} \rangle = \frac{1}{2} \delta_{J,J'} \delta_{M,M'} (1 + \zeta \zeta') K(\mathbf{p}') \{T_2 + \zeta \exp(-i\mathbf{p}' \cdot \mathbf{d}) T_1\}, \quad (4.11)$$

where the necessary conditions  $J=J'$  and  $M=M'$  for non-zero overlap come from the spinors in the initial and final states. By purposely making the choice  $J \neq J'$  the overlap of the initial and final states is zero, for all  $\mathbf{p}'$  and  $\psi(\mathbf{R})$ , and there is in the final state no remnant of the information in the initial state. Setting to zero the overlap of the initial and final states, and the overlap of the two states in the initial and final states, robs the model of correlations other than those due to the quantum exchange effects.

In (4.10) the matrix elements of the scattering length obey the selection rule  $J' = |J-1|, J$  and  $J+1$ , which is the selection rule for a tensor of rank one, namely, the spin  $\mathbf{I}$  in (4.6). Combining the desired orthogonality of the initial and final states with the selection rule one finds  $J' = |J-1|$  and  $J+1$ , and  $\zeta \zeta' = (-1)^{J+J'} = -1$ .

The kinematics of the scattering process is relatively simple. The duration of the collision is by design very small, so the potential energy of the struck particle is essentially the same in the initial and final states. On the other hand, the kinetic energy of the struck particle changes from  $(\hbar p)^2/2M$  to  $(\hbar p')^2/2M$ , and the conservation of momentum gives  $\mathbf{p}' = \mathbf{p} + \mathbf{k}$ . Moreover, measured on the scale of energy imparted to the struck particle, the energy of the other particle is essentially unchanged in the

scattering process. Hence, if the change in energy of the neutron is  $\Delta E$  the conservation of energy reads,

$$\Delta E + \frac{(\hbar p)^2}{2M} - \frac{(\hbar p')^2}{2M} = 0.$$

The recoil energy of the struck particle  $E_R = (\hbar k)^2/2M$ .

The total cross-section *per particle*, including the conservation of energy, is,

$$\frac{1}{2} \sum_{JM} \frac{1}{(2J+1)} w(J) \sum_{J' \neq J} \sum_{M'} |\langle \text{final} | V | \text{initial} \rangle|^2 \delta \left\{ \Delta E - E_R - \hbar^2 \frac{\mathbf{k} \cdot \mathbf{p}}{M} \right\}. \quad (4.12)$$

In this expression,  $w(J)$  is the weight attached to a state with angular momentum  $J = 0, 1, \dots, 2I$ , and,

$$\sum_{J=0}^{2I} w(J) = \sum_{J=0}^{2I} \frac{(2J+1)}{(2I+1)^2} = 1.$$

The factor  $1/(2J+1)$  in (4.12) accounts for the degeneracy of initial states with respect to the projection  $M$ .

From the definition of  $F(J' M', JM)$  in (4.10) one finds [3],

$$\sum_{J' \neq J} \sum_{M'} |F(J' M', JM)|^2 = (\sigma_{\text{inc}} / 4\pi) |T_2 + \zeta \exp(-i\mathbf{p} \cdot \mathbf{d}) T_1|^2 \left\{ 1 - \frac{J(J+1)}{4I(I+1)} \right\}, \quad (4.13)$$

where the so-called incoherent cross-section,

$$\sigma_{\text{inc}} = \pi I(I+1)B^2. \quad (4.14)$$

Note that the result (4.13) is independent of  $M$ , and hence in (4.12) the sum on  $M$  gives a factor  $(2J+1)$  which cancels with the associated degeneracy factor. Also, the result

(4.13) is zero for  $I = 0$ . On using (4.13) in the expression for the cross-section (4.12) the latter becomes,

$$(\sigma_{\text{inc}} / 8\pi) |K(\mathbf{p})|^2 \delta \left\{ \Delta E - E_R - \hbar^2 \frac{\mathbf{k} \cdot \mathbf{p}}{M} \right\} \sum_J w(J) |T_2 + \zeta \exp(-i\mathbf{p} \cdot \mathbf{d}) T_1|^2 \left\{ 1 - \frac{J(J+1)}{4I(I+1)} \right\}. \quad (4.15)$$

The presence in (4.15) of the phase factor  $\zeta = (-1)^J$  means there are for  $J$  even and odd different structure factors and cross-sections. Not surprisingly, the total cross-section is independent of the spatial phase-factor  $\exp(-i\mathbf{p} \cdot \mathbf{d})$  for,

$$\sum_{J(\text{even})} w(J) \left\{ 1 - \frac{J(J+1)}{4I(I+1)} \right\} = \sum_{J(\text{odd})} w(J) \left\{ 1 - \frac{J(J+1)}{4I(I+1)} \right\} = \frac{1}{4}. \quad (4.16)$$

Whence, the total cross-section per particle is,

$$\frac{1}{4} (\sigma_{\text{inc}} / 4\pi) |K(\mathbf{p})|^2 \delta \left\{ \Delta E - E_R - \hbar^2 \frac{\mathbf{k} \cdot \mathbf{p}}{M} \right\} \{ |T_1|^2 + |T_2|^2 \}. \quad (4.17)$$

This expression is different from the cross-section for Compton scattering by an isolated particle by a factor,

$$f = \frac{1}{4} (\sigma_{\text{inc}} / \sigma) \{ |T_1|^2 + |T_2|^2 \}, \quad (4.18)$$

where the single-atom cross-section,

$$\sigma = 4\pi \left\{ A^2 + \frac{1}{4} B^2 I(I+1) \right\}. \quad (4.19)$$

The value of  $f$  gives the shortfall in the cross-section due to the entanglement of spatial and spin degrees of freedom.



## 5. Discussion of the soluble model

Some aspects of the model introduced in section 4 can usefully be elaborated further. In the following, the conceptual features of the model will first be discussed. Thereafter, there is an orientation to the size of the shortfall in intensity due to quantum entanglement.

### 5.1 Exchange terms in neutron Compton scattering

It is important to stress again that the total final-state wavefunction (4.4) is a superposition. The particle labelled  $\alpha$  has an amplitude of equal magnitude at positions 1 and 2, and the same is valid for particle  $\beta$ . One does not know whether particle  $\alpha$  or  $\beta$  will be identified as the one recoiling out of its initial site. It is only through an interaction (a decoherence process) that the wavefunction is reduced such that one of the two states,

$$\exp(ip' \cdot \mathbf{R}_\alpha)\psi(\mathbf{R}_\beta) \quad \text{or} \quad \exp(ip' \cdot \mathbf{R}_\beta)\psi(\mathbf{R}_\alpha), \quad (5.1)$$

is selected.

The restoration of the cross-section with increasing  $\tau_s$  (cf. Fig. 1) to the size anticipated from standard experience is brought about by coupling to the environment, which is essentially frozen out on the time scale of the neutron Compton scattering experiments in question. Under standard conditions the identical particles are not in isolation from their environment, whereas they appear to be when viewed on a timescale  $\tau_s \sim 10^{-15}$  s. In other words, for the experiments in question the particles are in a pure state and described by a wavefunction. On increasing  $\tau_s$ , toward solid-state relaxation times, the pure state evolves through decoherence to a mixed state which can be described by a density matrix.

Next, we consider the physical significance of the integrals  $T_1$  and  $T_2$ . If we project the spatial part of the total final-state wavefunction (4.4) on to  $\varphi_j(\mathbf{R}_\beta)$ , say, the result is proportional to  $T_j^* \exp(i\mathbf{p}' \cdot \mathbf{R}_\alpha)$ . (In reaching this result one uses  $K_j(\mathbf{p}') \sim 0$  which is justified by the large magnitude of the final wavevector of the struck particle.) Hence, the probability for  $\beta$  to be in the state  $\varphi_j = \varphi_j(\mathbf{R}_\beta)$  while  $\alpha$  occupies the plane-wave state is the square of the absolute value of the projection of (4.4) on to  $\varphi_j(\mathbf{R}_\beta)$  and this quantity is found to have a value  $|T_j|^2/2$ . The scattering event does not select one of the two sites, and  $j = 1$  and  $j = 2$  are treated on an equal footing. Thus, on averaging over the two sites, we find that the probability that an initial state of the system is occupied after the reaction event created by Compton scattering is,

$$\frac{1}{2} \left\{ \frac{1}{2} |T_1|^2 + \frac{1}{2} |T_2|^2 \right\} = \frac{1}{4} \{ |T_1|^2 + |T_2|^2 \}. \quad (5.2)$$

This argument provides physical insight to one of the two factors in the intensity shortfall (4.18). The second factor is the appearance of  $\sigma_{\text{inc}}/\sigma$ ; here, the appearance of  $\sigma_{\text{inc}}$  is due in part to use of orthogonal initial and final states in the scattering event, and we have more to say on this aspect of the soluble model.

## 5.2 Orientation to the size of the shortfall in intensity

Let us start by considering the integrals  $T_1$  and  $T_2$ , defined according to (4.9). First, we can readily obtain an upper bound for their appearance in the cross-section (4.17) or (4.18). To this end, consider  $\psi(\mathbf{R})$  to be a linear combination of  $\varphi_1(\mathbf{R})$  and  $\varphi_2(\mathbf{R})$ . The coefficients in the linear combination are  $T_1^*$  and  $T_2^*$  and normalization of  $\psi(\mathbf{R})$  leads to  $|T_1|^2 + |T_2|^2 = 1$ . In general,  $\varphi_j(\mathbf{R})$  is one member of a complete set of wavefunctions. Expanding  $\psi(\mathbf{R})$  in terms of the complete sets for  $j = 1$  and  $j = 2$  one finds,

$$\{ |T_1|^2 + |T_2|^2 \} \leq 1. \quad (5.3)$$

Thus, the shortfall in the intensity (4.18) obeys  $f \leq \sigma_{\text{inc}}/4\sigma$ . For protons (deuterons) the maximum value of  $f$  is 0.24 (0.07).

If entanglement is lost during the scattering process, eq. (4.4) is not valid and the expressions for the cross-sections reduce to standard values for individual particles. The experimental data in Fig. 1 are reflecting such a situation where the cross-section is reduced for short times but reaches its conventional value for long times. The interpretation is that entanglement is lost after about 0.5 fs in the metal hydride materials NbH and PdH.

The value found for the shortfall in the cross section at short times for protons in NbH is about 30% (and somewhat larger for PdH). This corresponds to about 40% of maximum entanglement and a smaller degree (<10%) for deuterons in NbH. These numbers are only by way of orientation, because the assumption that entanglement is only set up pairwise should be seen as a first approximation. In reality, larger groups of correlated identical particles may be found at still shorter times. The model with pairwise entanglement might then be viewed as a limit existing shortly before the entanglement is broken. The entangled fraction will be set by competition between entanglement-creating forces and decoherence caused by the solid-state environment.

Equation (4.4) represents an extreme situation in the sense that the plane wave is assumed to be fully developed before decoherence occurs. In reality, there remains a spherical ( $l = 0$ ) component as a distance  $r$  travelled by the recoiling particle which is proportional to the magnitude of the Bessel function  $j_0(kr)/kr < 1/kr$ . At a typical distance of 0.5Å this fraction can be estimated to be of the order of a few percent.

Taking into account such deviations from the plane wave assumption does not impair the main conclusions of the model but has the consequence that the final state is not exactly orthogonal to the initial state but only approximately so. The same is true if the condition  $J' \neq J$  used to reach (4.18) is relaxed. It is illuminating to consider the result in the opposite extreme, namely when allowing all terms consistent with the

angular momentum coupling. One must consider separately  $I$  half-integer and  $I$  integer; on summing over all allowed  $\mathcal{J}$ , instead of eliminating terms  $J = \mathcal{J}$ , we have,

$$f = (1/2) (2I + 1)^{-1} \{I |T_1 + \exp(i\mathbf{p}\cdot\mathbf{d})T_2|^2 + (I + 1) |T_1 - \exp(i\mathbf{p}\cdot\mathbf{d})T_2|^2\}, \quad (5.4)$$

per proton in entangled proton pairs (half-integral particle spins), and

$$f = (1/2) (2I + 1)^{-1} \{(I + 1) |T_1 + \exp(i\mathbf{p}\cdot\mathbf{d})T_2|^2 + I |T_1 - \exp(i\mathbf{p}\cdot\mathbf{d})T_2|^2\}, \quad (5.5)$$

per deuteron in entangled deuteron pairs (integral particle spins). If we assume that  $\exp(i\mathbf{p}\cdot\mathbf{d}) \sim 1$  and that  $T_2 = T_1$  we find the values,

$$f = (1/2) |T_1|^2 = 1/4 \text{ for protons,} \quad (5.6)$$

$$f = (4/3) |T_1|^2 = 2/3 \text{ for deuterons,} \quad (5.7)$$

where the numerical values are obtained by taking  $|T_1|^2 = 1/2$ .

Such a modification of the original model calculation is but one of many which might be of use. It does not appreciably affect the outcome of our deliberation for protons (which scatter predominantly incoherently), but would confine the reduction factor for the deuterons between the two extreme limits 0.07, found with (4.18), and 0.67, found with (5.7).

## 6. Concluding Remarks

We have discussed the role of quantum entanglement in scattering, and reviewed the likelihood of it being the cause of the shortfall in intensity observed in neutron Compton scattering experiments performed on samples containing protons or deuterons. The key feature of the neutron Compton scattering experiments is the extremely short duration of the scattering event, which is typically less than a femtosecond in the

experiments under discussion. In this time domain, solid-state relaxation processes are essentially inoperative and quantum exchange correlations are the dominant force. This picture of physical processes is consistent with next to no dependence of the shortfall on the temperature of the sample, and restoration of the intensity to its expected value when the duration of the scattering event is increased and approaches solid-state relaxation times.

### **Acknowledgements**

We have benefited from discussions with Professor E. Balcar, Dr. M. Celli, Professor L. Pitaevskii, Dr. C. Simon and Dr. M. Zoppi. The hospitality of the directors of the Erwin Schrödinger Institute, Vienna, provided us the ideal venue in which to formulate ideas for the presentation.

### Figure caption

The ratio of the proton and niobium intensities in the Compton profile of the metallic hydride  $\text{NbH}_{0.85}$  is displayed, for two temperatures of the sample, as a function of the duration of the scattering event  $\tau_s$ . The full line is the expected value of the ratio, namely,  $\sigma_{\text{H}}/\sigma_{\text{Nb}} = 13.1$ , which the data approaches for the largest values of  $\tau_s$  [1].

## Appendix

We give here cross-sections for scattering neutrons of moderate energy by two identical particles. The essential feature of the present cross-sections, compared to cross-sections discussed in the main text, is that spatial components of the total initial and final wavefunctions are similar and look like (4.3). (In the extreme limit of Compton scattering the final spatial wavefunction must approach the result (4.4) and intensity accumulates at the recoil energy of one of the two particles.) We find it convenient to denote the spatial wavefunctions by  $\Psi$  and  $\Psi'$ ; the total wavefunctions are  $\Psi\chi_M^J$  and  $\Psi'\chi_M^{J'}$ , and  $\Psi$  ( $\Psi'$ ) depends on  $J$  ( $J'$ ).

Let  $\mathbf{R}_\alpha = \mathbf{R} + \mathbf{r}$  and  $\mathbf{R}_\beta = \mathbf{R} - \mathbf{r}$ . Cross-sections are different for  $J' = J$  and  $J' = |J-1|$  or  $J+1$ . For  $J' = J$ , the cross-section per particle is,

$$2\sum_J w(J)\left\{A^2 + \frac{1}{16}B^2J(J+1)\right\}\delta(\text{Energy})\left|\left\langle\Psi'\left|\exp(i\mathbf{k}\cdot\mathbf{R})\cos(\mathbf{k}\cdot\mathbf{r})\right|\Psi\right\rangle\right|^2. \quad (\text{A.1})$$

The argument of the delta function expresses conservation of energy in the scattering event and, in general, it depends on  $J$ . With  $J' = |J-1|$  or  $J+1$  the conservation of energy can depend on  $J'$  and  $J$ . The cross-section for these cases is,

$$2B^2I(I+1)\sum_J w(J)\left\{1 - \frac{J(J+1)}{4I(I+1)}\right\}\delta(\text{Energy})\left|\left\langle\Psi'\left|\exp(i\mathbf{k}\cdot\mathbf{R})\sin(\mathbf{k}\cdot\mathbf{r})\right|\Psi\right\rangle\right|^2. \quad (\text{A.2})$$

Matrix elements in (A1) and (A2) depend on the particular model used for the two particles, and little can be said apart from what is obvious in the way of general properties. Results (A1) and (A2) are similar to cross-sections for scattering by a homonuclear diatomic molecule [13].

## References

- [1] E. B. Karlsson, C. A. Chatzidimitriou-Dreismann, T. Abdul Redah, R. M. F. Streffer, B. Hjörvarsson, J. Öhrmalm and J. Mayers, *Europhys. Lett.* **46**, 617 (1999).
- [2] T. Abdul Redah, R. M. F. Streffen, C. A. Chatzidimitriou-Dreismann, B. Hjörvarsson, E. B. Karlsson and J. Mayers, *Physica B* **276 – 278**, 824 (2000).
- [3] E. B. Karlsson and S. W. Lovesey, *Phys. Rev. A* **61**, 062714 (2000).
- [4] L. Pitaevskii and S. Stringari, *Phys. Rev. Lett.* **83**, 4237 (1999).
- [5] C. A. Chatzidimitriou-Dreismann, T. Abdul Redah and J. Sperling, *J. Chem. Phys.* **113**, 2784 (2000).
- [6] C. A. Chatzidimitriou-Dreismann, T. Abdul Redah, R. M. F. Streffer and J. Mayers, *Phys. Rev. Lett.* **78**, 2839 (1997).
- [7] S. Ikeda and F. Fillaux, *Phys. Rev. B* **59**, 4134 (1999).
- [8] F. Fillaux, *Physica D* **113**, 172 (1998).
- [9] C. A. Chatzidimitriou-Dreismann, U. K. Krieger, A. Möller and M. Stern, *Phys. Rev. Lett.*, **75**, 3008 (1995)
- [10] R. M. Brugger, A. D. Taylor, C. E. Olsen, J. A. Goldstone and A. K. Soper, *Nucl. Instr. & Meth. in Phys. Research*, **221**, 393 (1984) .
- [11] C. Andreani, D. Colognese and E. Pace, *Phys. Rev. B* **50**, 10 008 (1999)
- [12] J. Hama and H. Miyagi, *Progr. Theor. Phys.* **50**, 1142 (1973)
- [13] S. W. Lovesey, *Theory of Neutron Scattering from Condensed Matter*, Clarendon Press, Oxford 1987.
- [14] A. C. Zemach and R. J. Glauber, *Phys. Rev.* **101**, 129 (1956).
- [15] E. Joos and H. D. Zeh, *Z. Phys. B* **59**, 223 (1985).



